ISSN 0010-9525, Cosmic Research, 2023, Vol. 61, No. 3, pp. 232–242. © Pleiades Publishing, Ltd., 2023.
Russian Text © The Author(s), 2023, published in Kosmicheskie Issledovaniya, 2023, Vol. 61, No. 3, pp. 230–241.

Coronal Propagation of Solar Protons during and after Their Stochastic Acceleration

I. Yu. Grigorieva[a], *, A. B. Struminsky[b], Yu. I. Logachev[c], and A. M. Sadovski[b]

[a] *Central (Pulkovo) Astronomical Observatory, Russian Academy of Sciences, St. Petersburg, 196140 Russia*
[b] *Space Research Institute, Russian Academy of Sciences, Moscow, 117997 Russia*
[c] *Skobeltsyn Institute of Nuclear Physics, Moscow State University, Moscow, 119991 Russia*
**e-mail: irina.2014.irina@mail.ru*

Received October 6, 2022; revised December 8, 2022; accepted December 12, 2022

Abstract—Solar protons in eruptive flares are stochastically accelerated in a wide spatial angle, and then they are effectively kept behind the expanding coronal mass ejection (CME) front, which can either bring protons to the magnetic-field line going to a remote observer or carry them away. We consider 13 solar proton events of cycle 24 in which protons with energy $E > 100$ MeV were recorded and were accompanied by the detection of solar hard X-ray (HXR) radiation with $E > 100$ keV by an ACS SPI detector and γ-radiation with $E > 100$ MeV by the FermiLAT telescope with a source in the western hemisphere of the Sun. The first arrival of solar protons into the Earth's orbit was determined in each event by a significant "proton" excess over the ACS SPI background during or after the HXR burst. All events were considered relative to our chosen zero time (0 min) of parent flares. The "early" arrival of protons to the Earth's orbit (<+20 min), which was observed in four events, corresponds to the "fast" acceleration of electrons (10 MeV/s). The "late" arrival of protons (>+20 min) corresponds to the "slow" acceleration of electrons (1 MeV/s) and was observed in six events. In three events, a "delayed" arrival of protons (>+30 min) was observed, when the CME propagation hindered the magnetic connection of the source with the observer. The direction of CME propagation is characterized in the catalog (SOHO LASCO CME Catalog) by the position angle (PA). The observed PA systematizes the times of the first arrival of protons and the growth rate of their intensity. The PA parameter should be taken into account in the analysis of proton events.

DOI: 10.1134/S0010952523700235

INTRODUCTION

The time of the arrival of the first solar protons (SP) in the Earth's orbit is one of the key parameters of a solar-proton event (SPE), which makes possible to estimate (within a model of proton propagation in the interplanetary medium) the first instant of their release from a source near the Sun to the magnetic-field line connecting the source to the observer. Knowing the time and location of proton release from the source, it is possible to make a choice in favor of one or another SP acceleration mechanism. The SP source is understood as the surface, crossing which the protons begin to propagate along the field lines of the Parker spiral in the solar wind. In propagation models, the source of solar cosmic rays (SCR) is described by the injection function $J(R, \Theta, \varphi, E, t)$, which specifies the number of particles emerging from a unit surface at point R into a spatial angle (Θ, φ) in the energy range dE per unit time dt. The SCR source is the result of the processes of acceleration and propagation of particles in the solar corona. Observational data show that the SCR source is long-lived and spatially distributed.

At present, there are two different views regarding where the SPs are accelerated (for example, [1–4]): in the lower corona during flares or high in the corona by the shock wave of a coronal-mass ejection (CME). Different acceleration processes imply different modes of propagation in the corona, i.e., different properties of sources (injection functions). An argument in favor of acceleration by the CME shock wave is the late arrival of SPs to the appropriate magnetic-field line relative to the flare time [5–7] and the large angular distance between the flare position and the base of the favorable field line or the site of generation of γ-radiation in behind the limb flares, for example, like September 29, 1989 [8]. To explain the same observational facts in the case of SP acceleration in flares with characteristic times and angular sizes that were considered small, the hypothesis of coronal SP propagation [9] and the hypothesis of long-term SP acceleration or capture in the posteruptive phase of flares [3, 10] were invoked.

Before the first FermiLAT observations of γ-radiation with $E > 100$ MeV, images of a possible SP source were not available. FermiLAT observations [11–13]

showed long-term γ-radiation with $E > 100$ MeV emerging directly from the flare region, which indicated SP interaction with the production of π_0 mesons in the solar atmosphere. This localization of γ-sources has become an additional argument in favor of the SP acceleration in flares. However, subsequent FermiLAT observations of γ-radiation with $E > 100$ MeV from behind the limb flares [14], when the angular distance between the flare and the source of γ-radiation was greater than 40° (similarly to [8]), again cast doubt on the flare origin of SPs [15, 16].

A separate class of SPEs consists of events accompanied by a ground-level enhancement (GLE) of intensity of secondary CRs recorded in the lower layers of the Earth's atmosphere. A CR cascade can be detected on the Earth's surface if the primary nucleon energy exceeds ~400 MeV (atmospheric cutoff threshold) and the average energy of solar protons in the spectrum is >1 GeV. Since the propagation effects are minimal at high SP energies, it is believed that the GLE onset most accurately indicates the time when protons exit the source into interplanetary medium (IPM) (according to the estimates of [4], the SP propagation time error is ±1 min). The atmospheric cutoff threshold only slightly exceeds $E = 266$ MeV, which is the threshold energy for the generation of π_0 mesons. Therefore, cases of detection of γ-radiation with $E >$ 100 MeV (FermiLAT) and GLE events should correlate with each other if the same population of particles interacts on the Sun and in the Earth's atmosphere, i.e., under favorable propagation conditions and one acceleration mechanism.

The γ-radiation maxima with $E > 100$ MeV recorded by FermiLAT coincide with the HXR radiation maxima in the energy range 100–300 keV recorded by FermiGBM within a few seconds. This coincidence implies a single process of acceleration and propagation of both ions (protons) and electrons [13]. It also turned out that the time profiles of electrons and protons with comparable relativistic factors (the ratio of the particle velocity to the speed of light V/c) are similar [17, 18], and relativistic electrons with $E \sim 10$ MeV cannot be accelerated by shock waves [19]. It follows from the above that the acceleration of protons by CME shock waves cannot be the predominant mechanism of energy gain [17, 18], otherwise GLE events would be observed much more frequently.

In our opinion, solar electrons with $E > 1$ MeV and protons with $E > 100$ MeV are accelerated stochastically (in a multitude of elementary acts with characteristic times much shorter than the entire acceleration process) in eruptive flares with a duration of more than 10 min against the background of CME acceleration (the time of maximum energy release) [20]. The beginning of the CME acceleration can be considered as the beginning of an increase in the emission measure in the presence of radio emission at frequencies below 1415 MHz [21, 22].

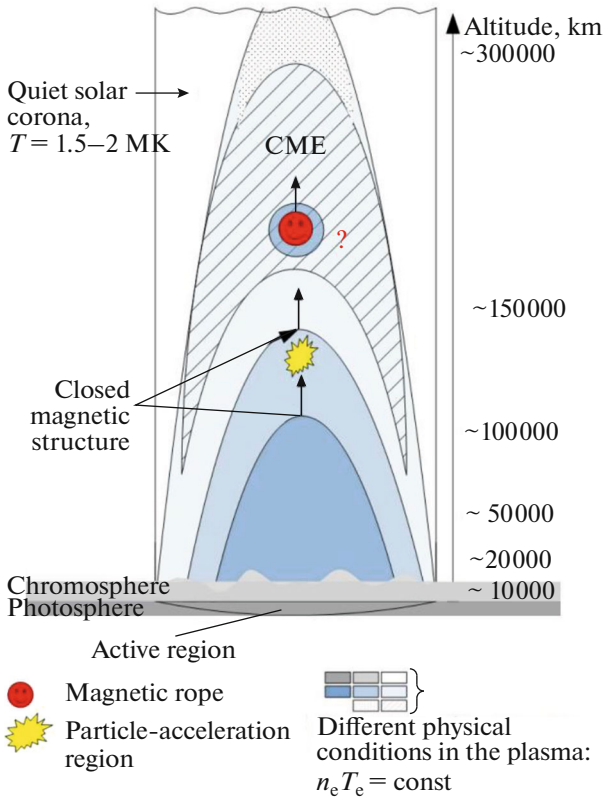

Fig. 1. Scheme of the development of an eruptive flare according to our view.

The traditional approach to the search for the acceleration mechanism is as follows: knowing the time and location of proton exit from the source, one can make a choice in favor of one or another SP acceleration mechanism [4]. On the other hand, by specifying certain (physically substantiated) properties of the acceleration process on the Sun, one can search for confirmation of the chosen acceleration process in SCR observations in the IPM and specify the details of the propagation processes in the corona and in the IPM. This is the approach used in our work.

PROPERTIES OF THE SOURCE OF SOLAR PROTONS UNDER STOCHASTIC ACCELERATION

Figure 1 shows an approximate scheme of the development of an eruptive flare according to our views with the designation of characteristic altitudes. The maximum angular size of the loop system is the size of the maximum magnetic dipole during the flare (with successive involvement of dipoles of different sizes from smaller to larger in the flare process). In this case, accelerated particles easily fill an increasingly larger spatial angle, which is coronal propagation during the stochastic acceleration.

Study [17] is based on the idea that the simultaneous acceleration of electrons and protons should not violate the condition of electrical neutrality of plasma and so the number of electrons and protons accelerated to the same velocities should be comparable. In this case, a "proton" flare (appearance of interacting protons with $E > 10$ MeV) should begin at a plasma electron temperature of ~17 MK (protons with $E \sim 3$ MeV are equivalent in velocity to electrons with $E \sim 1.5$ keV), and the start of generation of π_0 mesons will be possible at an electron energy of ~150 keV (protons with $E \sim 300$ MeV are equivalent in velocities to electrons with $E \sim 150$ keV), i.e., against the background of HXR radiation with $E > 100$ keV.

There are observational data that show the acceleration time of electrons to a kinetic energy of ~100 keV on the order of ~400 ms [19]. There are also delays between HXR bursts at different electron energies (20, 50, 100, 200, and 300 keV) on the order of tens of milliseconds, which may be due to the acceleration time (see review [23] and references therein). Therefore, the time required for protons to reach $E \sim 200$ MeV will be ~1 min when electrons are accelerated to a kinetic energy of ~100 keV in 40 ms ("fast" acceleration) or ~10 min when electrons are accelerated to ~100 keV in 400 ms ("slow" acceleration). If the onset of microwave radiation at 8.8–15.4 GHz is taken as zero time in solar events (it usually coincides with the appearance of a significant signal of HXR radiation with $E \sim 100$ keV), the expected time of arrival of protons with $E \sim 200$ MeV ($V/c = 0.57$) to the Earth's orbit will be ~11 min (~21 min, respectively) when propagating without scattering along the Parker spiral to the Earth (1.3 AU, with the solar-wind speed being 300 km/s). Thus, the uncertainty of the characteristic time of solar electron acceleration up to $E \sim 100$ keV determines the uncertainty of the time of the first arrival of SPs with $E \sim 200$ MeV to the Earth's orbit and is about 10 min.

Also, when the first arrival of SPs is detected by energy-integrated detectors, there is an uncertainty in the time of the first arrival of SPs associated with the velocity dispersion. Let us estimate the maximum proton acceleration time from $E \sim 100$ to ~500 MeV, which will allow protons with $E \sim 500$ MeV ($V/c = 0.75$) to arrive before protons with $E \sim 100$ MeV ($V/c = 0.43$). When propagating without scattering along the Parker spiral to the Earth (1.3 AU, with the solar-wind speed being 300 km/s), the propagation time of protons with $E \sim 500$ MeV ($V/c = 0.75$) will be ~15 min, and for protons with $E \sim 100$ MeV ($V/c = 0.43$) it will be ~25 min. Thus, the maximum acceleration time for protons with E from ~100 to ~500 MeV must be less than ~10 min for the velocity dispersion not to be observed.

These estimates determine the choice of zero time for the analysis of phenomena associated with solar flares, as well as the criteria for "early" (<+20 min) and "late" (>+20 min) arrival of SPs into the Earth's orbit relative to zero time. In the case of a "fast" mode of electron and proton acceleration, the first SPs with $E > 100$ MeV will be observed on Earth 10 min after our chosen zero point (possibly, simultaneously or later than protons with $E > 500$ MeV). In the case of a "slow" mode of electron and proton acceleration, the first SPs with $E > 100$ MeV will be observed on Earth in 20 min. Both options can potentially be accompanied by a GLE, but at different times relative to the chosen zero.

The estimate of the proton-acceleration region (with angular size φ, the source of γ-radiation with $E >$ 100 MeV) will be $\varphi \approx 2\arccos(R_0^{-1})$ of approximately 49°–74°, where $R_0 = (1.1 - 1.25)\,R_S$ is the heliocentric distance to the maximum altitude of the development of the flare event (the CME breakaway point), and R_S is the solar radius. Indeed, GLE events are observed in the latitude range of ±30° from the equator [24], which apparently corresponds to height of the proton source $H \sim 0.15\,R_S \sim 110$ Mm. These estimates agree with the results of the statistical analysis [25], which showed that the longitudinal distribution of GLE events is approximated by a Gaussian in the range of longitudes from ~E 90° to ~W 150° with a maximum at ~W 60°, which almost coincides with the nominal position of the base of the favorable field line ~W 55° in a quiet solar wind.

Traditionally, such spatially distributed sources are associated with acceleration on CME shock waves rather than acceleration of particles in the magnetosphere of the active region, where intense energy release (multiple reconnection) occurs, accompanied by CME acceleration. Both in the case of acceleration by shock waves and during stochastic acceleration in flares, protons are kept behind the CME front, and the size of the SP source increases as the CME accelerates, but the nature of the acceleration is different [17, 18, 20]. In any scenario, the coronal propagation of SCRs is the result of an increase in the spatial angle of the CME front in powerful eruptive flares (the formation of Halo-type CMEs). The development of our hypothesis of the origin of SPs lies in the fact that the CME is capable of both bringing accelerated protons to the field line directed to the observer and carrying them away. In this case, the direction of CME propagation, which is characterized by parameter PA (position angle) measured from north in a counterclockwise direction. The CME propagates in the plane of the ecliptic of the western solar hemisphere at PA ~ 270°. The angle values other than this worsen the conditions for the SP propagation.

The observed delay in the first arrival of SPs relative to the above estimates and the slow increase in their intensity correspond to the late crossing of the favorable field line by the region of proton sources and difficult access to it in the future (transfer of the SPs across the field lines). In this case, it is necessary to

speak about both the longitudinal and latitudinal coronal propagation of CMEs and SPs. The time of the first detection of SPs depends on the background count of the detector and the rate of increase in the intensity of the proton flux at the observation point. The late arrival and the slow increase in intensity can have the same cause—the presence of obstacles for the exit of particles to a favorable field line. The CME front can be such an obstacle.

Considering various proton events accompanied by FermiLAT detection of γ-radiation with $E > 100$ MeV [26], it is easy to find cases in which the times of the first arrival of SPs relative to the onset of CME acceleration differ significantly with almost the same location of parent flares relative to the Earth, taking into account the possible width of the SP source. At the same time, judging by the videos of the LASCO coronagraph in the public domain, the early arrival of SPs corresponds to the initial propagation of CMEs in the ecliptic plane, and their delayed arrival corresponds to the initial propagation of CMEs outside the ecliptic plane. In addition, we take into account the influence of the position of the flare on the solar disk, the direction of CME propagation during the first arrival of the SPs to the Earth's orbit, and the growth rate of their intensity in the selected events.

TOOLS AND SELECTION OF EVENTS

We have considered the list of events from [28]. The study included all 13 SPEs of solar cycle 24 from the western solar hemisphere in which protons with $E > 100$ MeV were detected, the parent flares of which were accompanied by γ-radiation with $E > 100$ MeV [26–28]. The conclusions drawn in our study on the basis of 13 events of cycle 24 are verified using the examples of the last GLE event of cycle 23 (December 13, 2006 [29, 30]) and the first GLE event of the current cycle 25 (October 28, 2021 [31, 32]). Most of the events that we selected were already studied by other authors, but they advocated the SP acceleration by the CME shock wave, for example, [16, 33, 34].

The main characteristics of events relative to zero time are given in Table 1; the solar data are taken from the files YYYYMMDDevents.txt (https://cdaw.gsfc.nasa.gov/CME_list/NOAA/org_events_text/). As a result, the events selected for the study included: the only two GLE events of cycle 24 (GLE 71 on May 17, 2012 [20, 27, 33, 34], and GLE 72 on September 10, 2017 [17, 35, 36]); eight events associated with known flares or SPEs (M3.7 on March 7, 2011 [11, 13, 21], M2.5 on June 6, 2011 [11, 13], X6.8 on August 9, 2011 [18, 20, 22, 33, 34], X1.7 on January 27, 2012 [33, 34], X1.1 on July 6, 2012 [33, 34], January 6, 2014 [14, 37], January 7, 2014 [38], and X9.3 on September 6, 2017 [17, 21, 28]; one event each from cycles 23 and 25 and three little-known SPEs from cycle 24 (one of them is the event of June 25, 2015 [28], which is not on any of the graphs, since the onset of the proton increase was later than +60 min). All events are analyzed relative to the selected zero time—the onset of microwave radio emission at frequencies of 8.8 or 15.4 GHz, just as we did, for example, in [17, 18, 20, 21]. In the absence of data at these frequencies, other available data are taken as zero; for example, the onset of type II radio emission is taken for the behind-the-limb event on January 6, 2014. For the event of October 28, 2021, in which microwave radiation apparently did not exceed the threshold detection intensity (https://cdaw.gsfc.nasa.gov/CME_list/NOAA/org_events_text/), the onset of radio emission at 610–245 MHz is selected as zero time.

The time of the first arrival of SPs into the Earth's orbit is considered as the onset of a significant increase in the count rate of the anticoincidence shield of the spectrometer on the *INTEGRAL* satellite (ACS SPI) concurrently or after a burst of solar HXR radiation [17, 18, 20, 21, 29]. The ACS SPI detector records HXR radiation with $E > 100$ keV and protons with $E > 100$ MeV and is an efficient but not calibrated detector. The ACS SPI data are available online (https://isdc.unige.ch/~savchenk/spiacs-online/spiacspnlc.pl) with a time resolution of 50 ms. With 1-min smoothing and background subtraction, the ACS SPI count rate of less than ten counts per 50 ms becomes significant. We use the ACS SPI detector to study the relationship between solar flares and proton events.

The CME information is taken from the SOHO LASCO CME Catalog (https://cdaw.gsfc.nasa.gov/CME_list/). Our table shows the times of the first and second times of detection of the position of the CME (t_1 and t_2), its average velocity V_{av}, and the velocity of propagation from the first to the second recorded position V_{12}, as well as the PA for these time points. The fields of view of LASCO coronagraphs C2 and C3 overlap, but coronagraphs C2 and C3 do not take frames simultaneously, so the time between t_1 and t_2 may not match the frame duty cycle of 12 min.

RESULTS AND DISCUSSION

The division of events into "fast" and "slow" according to the character of the intensity increase is explained in Fig. 2. The early arrival of protons corresponds to the expected arrival of protons with $E \sim 200$ MeV during propagation without scattering between +10 and +20 min in the case of "fast" acceleration. The behind-the-limb event of January 6, 2014, with a GLE on one neutron monitor (NM)—subGLE [37]—shows that an "early" arrival of protons at +13 min with an unfavorable location of the flare (it is necessary to traverse more than 40° to the east in longitude to reach a favorable field line) is possible. Therefore, all proton enhancements with time profiles "to the right" of the proton event profile on January 6, 2014, will be considered "slow," and "to the left" will be considered "fast."

Table 1. Some characteristics of solar-proton arrival events

No.	A	B	C min	D min	E min km/s	F deg	G < ≈ >
1	**Dec. 13, 2006 02:21 UT**	**S06W35 X3.4**	**+17.5**	**+28**	**+33/+57 1774/1869**	**193/192**	**S6 < S77**
2	**Mar. 7, 2011 19:47 UT**	**N24W60 M3.7**	**>+45**	**No**	**+13/+25 2126/1845**	**315/311**	**N24 < N45**
3	June 7, 2011 06:25 UT	S21W54 M2.5	+20	No	+24/+31 1255/1655	238/247	S21 < S32
4	Aug. 4, 2011 03:49 UT	N19W36 M9.3	+25	No	+23/+29 1316/1547	296/289	N19 < N26
5	**Aug. 9, 2011 08:01 UT**	**N17W69 X6.8**	**+10**	**No**	**+11/+23 1610/2202**	**279/279**	**N17 > N9**
6	Sep. 6, 2011 22:20 UT	N14W18 X2.1	+26	No	+45/+52 575/908	295/286	N14 < N25
7	Jan. 27, 2012 18:10 UT	N27W71 X1.7	+20	No	+17/+28 2505/1793	292/294	N27 ≈ N22
8	**May 17, 2012 01:30 UT**	**N13W87 M5.1**	**+10**	**+13**	**+18/+30 1582/1757**	**268/264**	**N13 > S02**
9	July 6, 2012 23:03 UT	S17W50 X1.1	+20	No	+21/+27 1829/3278	237/227	S17 < S33
10	**Jan. 6, 2014 07:45 UT**	**S08W110** [14]	**<+13**	**+13** [37]	**+15/+27 1400/1757**	**261/267**	**S8 ≈ S9**
11	**Jan. 7, 2014 18:05 UT**	**S15W11 X1.2**	**+45**	**No**	**+19/+31 1831/2234**	**231/231**	**S15 < S39**
12	**June 25, 2015 08:12 UT**	**N09W42 M7.9**	**No**	**No**	**+24/+36 1627/2030**	**323/327**	**N9 < N53**
13	Sep. 6, 2017 11:54 UT	S09W42 X9.3	+26	No	+30/+36 1569/2050	205/205	S9 < S65
14	**Sep. 10, 2017 15:52 UT**	**S09W91 X8.2**	**+20**	**+16**	**+8/+14 3163/4061**	**260/260**	**S9 ≈ S10**
15	Oct. 28, 2021 15:27 UT	S26W05 X1.0	+20	+23	+21/+33 1520/1934	189/190	S26 < S81

Note. The cases of early SP arrival (the time of the first detection of protons <+20 min) are marked in bold; the rest are the cases of the late SP arrival (the time of the first detection is <+30 min). A, date and the chosen zero time; B, active region coordinates and flare strength (*GOES*); C, onset of proton increase in ACS SPI; D, onset of a GLE event; E, times of the first and second frame of the CME (SOHO LASCO, minutes after 0), average velocity, and velocity of the first appearance of the CME (km/s); F, CME position angle (PA, deg) on the first and second frames (SOHO LASCO); and G, comparison of solar-flare latitude and angle difference (PA = 270°): < CME worsens the propagation conditions, > improves, ≈ does not change.

The event of January 7, 2014, is an example of a "late" arrival and a "slow" increase in intensity. It is symmetrical to the January 6, 2014, event relative to the favorable field line of the source (S15W11, it is necessary to traverse more than 44° to the west in longitude), but the CME propagates in an unfavorable direction (PA = 239°). A pair of non-GLE events on August 4, 2011, and September 6, 2011 (for almost the same flare coordinates on the disk and PA angles), shows a delay of ~5 min relative to the expected arrival of +20 min (i.e., +25 min); these are events with "slow" acceleration. Also, the time profiles of the response to the arrival of protons at the ACS SPI for this pair repeat each other until approximately +32 min; later, the SP intensities in the event on August 4 began to grow faster than on September 6. This may be due to the difference in the acceleration rates in the posteruptive phase (the CME velocity on September 6 was the lowest of the entire sample of events).

Figure 3 shows the ACS SPI time profiles for six events conditionally divided into two groups according to the effect of CME on SP propagation. Panel 3a focuses on the HXR flare emission. The maximum intensities of HXR emission differ among flares by

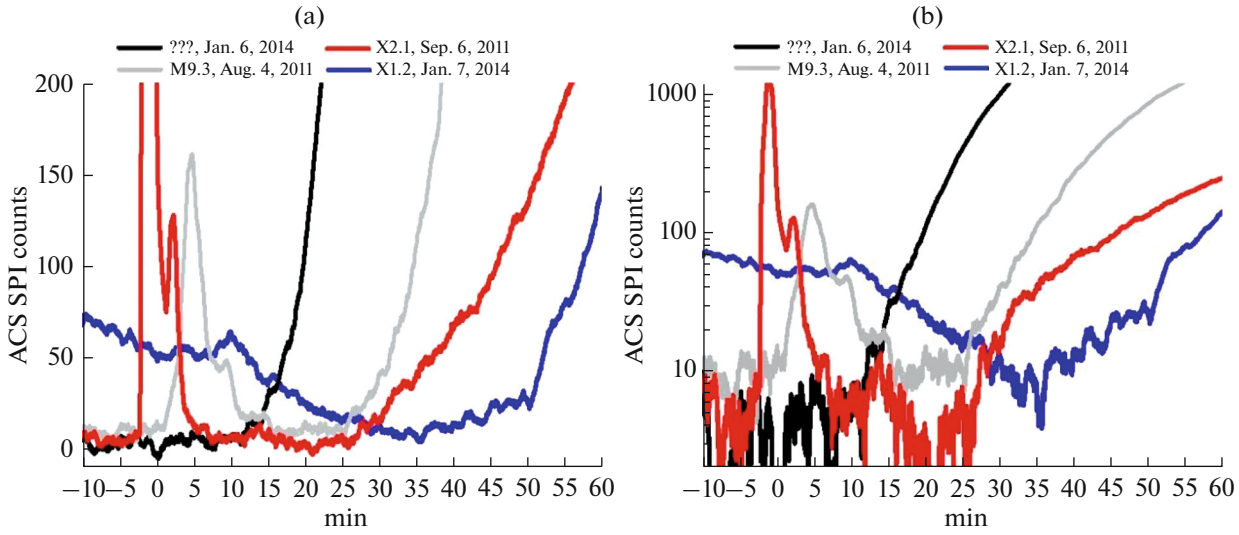

Fig. 2. Time profiles of the ACS SPI count rate for 50 ms (1-min smoothed averages, background subtracted) in events 4, 6, 10, and 11 (according to Table 1). Panels (a) and (b) differ in vertical scale.

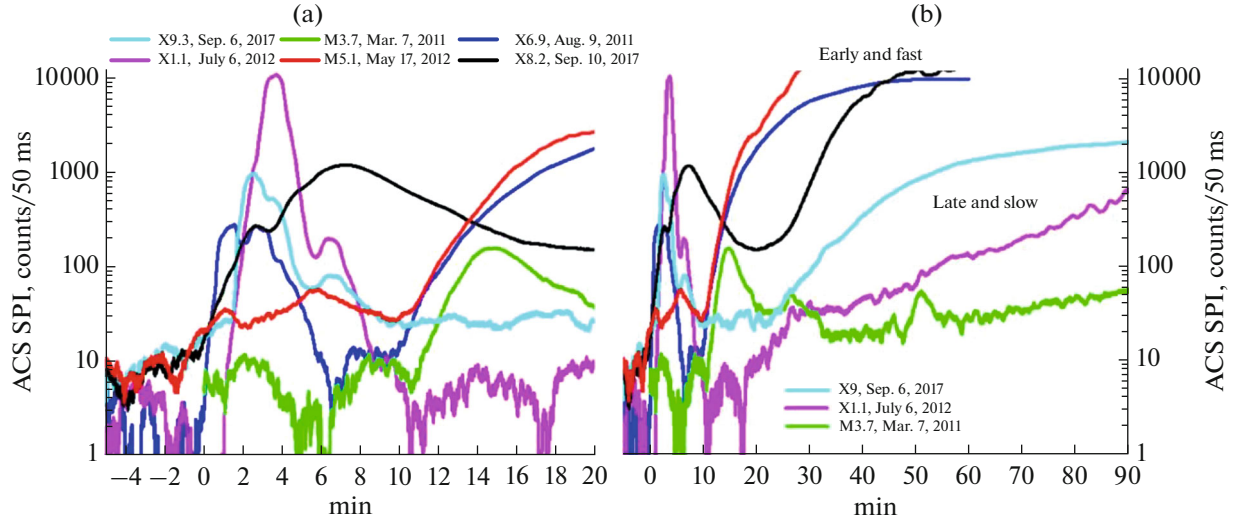

Fig. 3. Time profiles of the ACS SPI count rate over 50 ms (1-min smoothed averages, background subtracted) in events 5, 8, and 14 with favorable PA and 2, 9, and 13 with unfavorable PA (according to Table 1, Fig. 4). Panels (a) and (b) differ in horizontal scale.

more than two orders of magnitude, but the temporal dynamics of HXR emission (i.e., flare energy release) in these events is similar for the first 6–8 min. We associate this time interval, when the "synergy" of flares and CMEs occurs [39], with the stochastic acceleration of relativistic electrons and protons with $E > 100$ MeV and CME acceleration in the lower corona [17, 20–22]. The concept of "synergy" between flares and CMEs appears to be confirmed by the latest FermiLAT observations of the behind-the-limb flare on July 17, 2021 (S20E140), STIX aboard *Solar Orbiter* and *STEREO-A* (Fig. 3 in [40]). The first ideas about the need to take the CME acceleration into account when considering SPEs were expressed in [33, 34]. The gradual event on March 7, 2011, in which the main HXR burst was known to be in the posteruptive phase of the flare, is of particular note [21].

Figure 3b focuses on the differences in the times of the first arrival of protons and the rate of increase in their intensity (according to the ACS SPI data) in the SPEs under consideration. The character of the increase in the SP intensity is determined by the function of SP injection onto a favorable field line. The curves that show early and fast growth have a favorable PA, while the curves that showing late and slow growth have an unfavorable PA. Thus, we have identified two groups of events that are characterized by (1) early arrival of protons and a rapid increase in their intensity

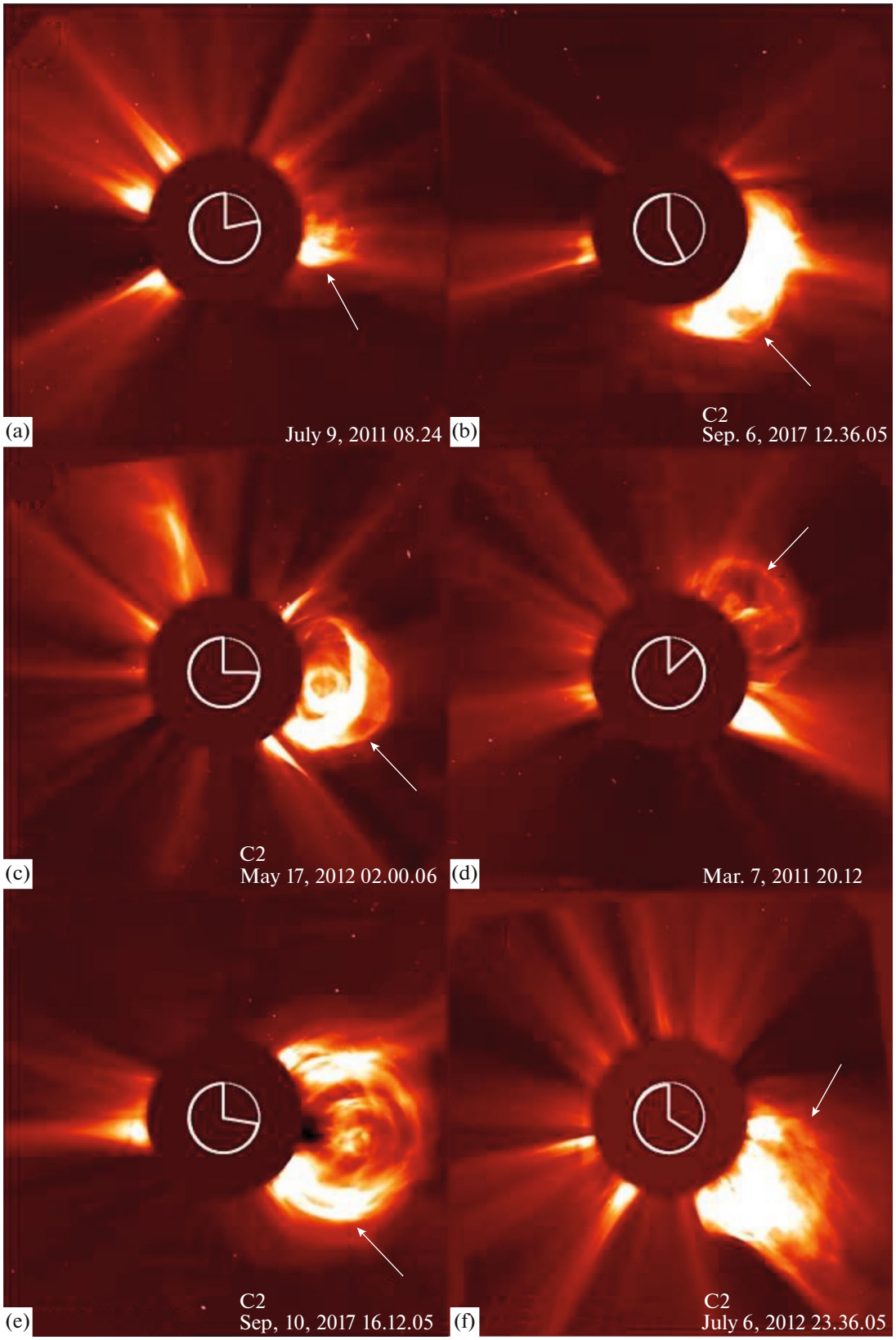

Fig. 4. The second frame of the CME observation in the LASCO C2 field of view: left panels (a, c, e) show favorable CME propagation; right panels (b, d, f) show unfavorable CME propagation (see Fig. 3, Table 1).

(favorable PA) and (2) delayed (late) arrival of protons and a slow increase in their intensity (unfavorable PA). These groups have almost no difference from each other in velocities V_{av} and V_{12} (see Table 1), but they differ in the flare coordinates and PA value. It should be noted that $V_{av} > V_{12}$ (see Table 1) only in the case of two long gradual flares on March 7, 2011, and January 27, 2012, when the CME acceleration [8] should be definitely present before, during, and after the observed HXR emission.

The CME propagation directions (SOHO LASCO C2) are shown in Fig. 4. The second frames of the CME propagation in six events of the 24th cycle from Fig. 3 are shown. Three horizontal rows differ in the properties of parent flares in soft X-ray (SXR) radiation: (a, b) pronounced impulsive phase, (c, d) no impulsive phase (gradual flare), and (e, f) weakly pronounced impulsive and prolonged posteruptive phases of the flare. The circles and radii on the panels of Fig. 4 show the PA value. The arrows show which phenomena are identified with CMEs in the frames. Maximum velocities of CMEs in the field of view of LASCO C2 were reached in cases (e, f), but this did not lead, as might be expected, to an earlier arrival of protons from the point of view of the authors of [35]. The observed PA systematizes the times of the first arrival of protons and the growth rate of their intensity. In cases of early arrival of protons and a rapid increase in their intensity, the CME propagated mainly in the ecliptic plane (PA ~ 270°), and in cases of delayed (late) arrival and slow growth, outside the ecliptic plane.

Figure 5 shows the events of December 13, 2006 (GLE 70, cycle 23 [29, 30]), and October 28, 2021 (GLE 73, cycle 25 [31, 32, 42–44]). The December 13 proton event (GLE 70, see Table 1) contradicts the proposed interpretation of observations based on the six events in Figs. 3 and 4, which is why it is called Maverick [41]. The value of PA = 193° (unfavorable angle) corresponds to the delayed arrival of protons, although the time of the onset of the proton enhancement on the ACS SPI (taking into account the X-ray background) is relatively early, +16.5 min [29]. Perhaps this is due to the complex character of the eruption [30] and the absence of LASCO observations in this event until +33 min (https://cdaw.gsfc.nasa.gov/CME_list/). In the case of the October 28 proton event (GLE 73, see Table 1), the position of the active region on the solar disk (S26W02) does not allow us to unambiguously identify the late arrival of protons and the slow increase in their intensity with PA = 189°. In these two events, the PA values are similar, and one can speculate by attributing the observed difference in first arrival times to the longitudinal propagation of protons.

The other two events in Fig. 5—June 6, 2011, and January 27, 2012—are non-GLE events for which the first arrival of protons at +20 min is expected. The position of the flares and the direction of CME propagation relative to the ecliptic in them were symmetrical (S21W54 (S21 < S32) and N27W71 (N27 ≈ N22), respectively, see Table 1). The difference in the flare longitudes fits into our estimates of the size of the SP source. The slowest growth of the ACS SPI signal in Fig. 5 is for the event of October 28, 2021 (S26 < S81, see Table 1).

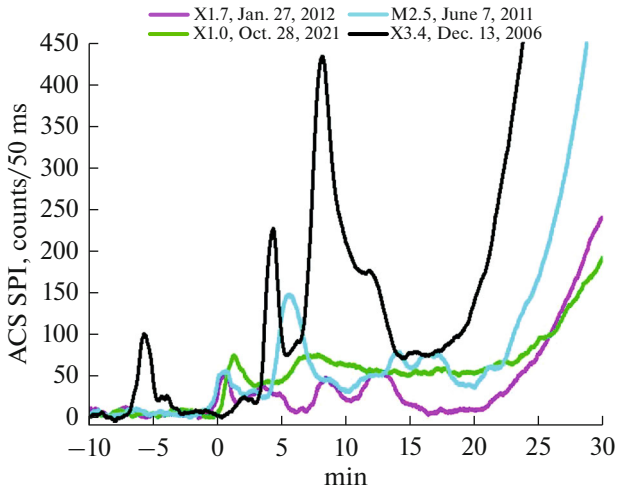

Fig. 5. Time profiles of the ACS SPI count rate over 50 ms (1-min smoothed averages, background subtracted) in events 1, 3, 7, and 15 (according to Table 1).

Figure 6 compares all GLE events considered in our study with the non-GLE event on August 9, 2011 [18, 20], and the sub-GLE event on January 6, 2014 [36, 37]. This is important, as the August 9 event (without GLE) is an example of the fastest development of the proton increase (arrival of protons at +10 min), while sub-GLE (from a source behind the limb) is expectedly slow (Fig. 6a). It should be noted that the fastest arrival of protons was in GLE 69 on January 20, 2005 [3, 45], at +8 min, if we choose the zero time (06:40 UT) to be the same as in [29]. We did not include this event in the table due to poor CME observations at LASCO.

The pair of August 9, 2011, and May 17, 2012, was considered in detail in [20], where it was shown that, on August 9, there was not enough time to accelerate the required amount of protons to relativistic energies to generate GLE. However, in these events, protons with E ~ 100–500 MeV entered the IPM earlier than +10 min; i.e., the acceleration mode was the "fastest."

In all the four GLEs and one sub-GLE considered, the first arrival of protons occurred before +20 min (in GLE 72 according to the NM data), which corresponds to the "fast" acceleration regime. However, the growth rates of the proton intensity differed. The rate indicates the injection function, which depends on the acceleration mode and the propagation process in the corona. In Fig. 6b, the growth rate does not initially determine the maximum values; a long-term and

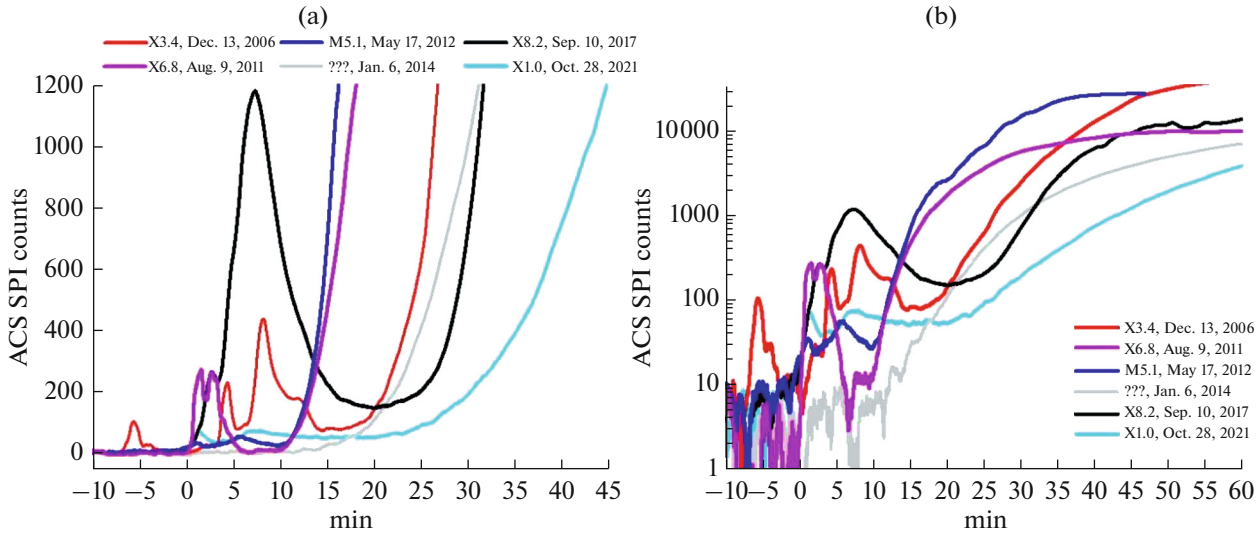

Fig. 6. Time profiles of the ACS SPI count rate over 50 ms (1-min smoothed averages, background subtracted) in GLE 70, 71, 72, and 73 (according to Table 1, rows 1, 8, 14, and 15), subGLE (according to Table 1, row 10), and non-GLE event (according to Table 1, row 5).

gradual injection onto the field line in the IPM is required. The characteristics (amplitudes) of increases in HXR radiation are not related to the characteristics of proton fluxes in the heliosphere.

A look at the SP sources during acceleration by the CME shock wave is described for GLE events of the 23rd cycle in [46] and other significant GLE events in [47]. The studies with the same ideas about SP acceleration based on the events of the 24th cycle are cited above [16, 24, 33–35, 37, 38]. The main conclusions [46, 47] are that particle acceleration and escape into the IPM occur at heliocentric distances of $2–4R_S$ in a wide spatial angle (up to 100°) in longitude. The source height increases with the spatial angle. In our qualitative model of the development of eruptive flares, particles are accelerated at heights up to ~$1.25R_S$, and their main release to a favorable field line occurs when they cross the shock-wave front, same as in [46, 47]. Insignificant proton fluxes can reach a favorable field line earlier due to transverse diffusion.

CONCLUSIONS

The introduction of a conditional zero time for solar flares (the onset of radio emission at frequencies of 8.8–15.4 GHz) and the assumption of the necessary time for electron acceleration to an energy of ~100 keV (tens or hundreds of milliseconds) made it possible to order and classify the ACS SPI proton enhancements.

• "Fast" acceleration of electrons (tens of milliseconds) corresponds to the "early" arrival of protons to the Earth's orbit (<20 min) relative to the selected zero time (events 1, 5, 8, 10, and 14 in Table 1). When the duration of stochastic proton acceleration is >10 min, protons can be accelerated to relativistic energies and, therefore, "early" (<20 min) GLE can be realized given a sufficient amount of SPs.

• "Slow" acceleration of electrons (hundreds of milliseconds) corresponds to the "late" arrival of protons (>20 min) (events 3, 4, 6, 7, 9, 13, and 15 in Table 1). When the duration of the stochastic acceleration of protons is >20 min, it is possible for them to reach relativistic energies and realize a "late" (>20 min) GLE given a sufficient amount of SPs.

• In any mode of electron acceleration in a large volume occupied by an eruptive flare, an SP source with large angular dimensions (i.e., coronal propagation) is realized.

• "Delayed" arrival of protons (>30 min, events 2, 11, and 12 in Table 1) is a consequence of the worsening of propagation conditions (i.e., coronal capture with an unfavorable direction of CME propagation), while propagation conditions in the IPM remain almost unchanged.

• The direction of CME propagation is characterized in the field of view of the LASCO coronagraph by the position angle (PA). The PA parameter must be taken into account in the analysis of proton events.

ACKNOWLEDGMENTS

This study was prepared on the basis of three reports of the authors at the 37th All-Russian Conference on Cosmic Rays in memory of M.I. Panasyuk, June 27–July 2, 2022, at the Skobeltsyn Institute of Nuclear Physics, Moscow State University. The authors are grateful to the organizers of the conference for the opportunity.

The CME catalog is generated and maintained at the CDAW Data Center by NASA and the Catholic University of America in cooperation with the Naval Research Labo-

ratory. SOHO is a project of international cooperation between ESA and NASA.

This work is based on INTEGRAL public data provided by Dr. V. Savchenko through the INTEGRAL Science Data Centre infrastructure hosted at the University of Geneva. This work is based on observations with INTEGRAL, an ESA project with instruments and a science data center funded by ESA member states (especially the PI countries: Denmark, France, Germany, Italy, Switzerland, and Spain) and with the participation of Russia and the United States. The ACS SPI detector system has been provided by the MPE Garching/Germany.

FUNDING

The study was supported by subsidies on the topics "Plasma" (A.B. Struminsky and A.M. Sadovski) at the Space Research Institute, Russian Academy of Sciences, and "MAS" (I.Yu. Grigorieva) at the Central Astronomical Observatory, Russian Academy of Sciences.

CONFLICT OF INTEREST

The authors declare that they have no conflict of interest.

REFERENCES

1. Cliver, E.W., History of research on solar energetic particle (SEP) events: The evolving paradigm, *Universal Heliophysical Processes Proc. IAU Symposium no. 257,* Gopalswamy, N. and Webb, D.F., Eds., 2008, pp. 401–412. https://doi.org/10.1017/S1743921309029639
2. Miroshnichenko, L.I., Solar cosmic rays: 75 years of research, *Phys.-Usp.,* 2018, vol. 61, no. 4, pp. 323–352. https://doi.org/10.3367/UFNe.2017.03.038091
3. Klein, K.-L., Radio astronomical tools for the study of solar energetic particles II. Time-extended acceleration at subrelativistic and relativistic energies, *Front. Astron. Space Sci.,* 2021, vol. 7, p. 580445. https://doi.org/10.3389/fspas.2020.580445
4. Kahler, S.W., Hildner, E., and van Hollebeke, V.A.I., Prompt solar proton events and coronal mass ejections, *Sol. Phys.,* 1978, vol. 57, pp. 429–443.
5. Bazilevskaya, G.A., On the early phase of relativistic solar particle events: Are there signatures of acceleration mechanism?, *Adv. Space Res.,* 2009, vol. 43, no. 4, pp. 530–536. https://doi.org/10.1016/j.asr.2008.08.005
6. Kahler, S.W., Sheeley, N.R., Jr., Howard, R.A., et al., Associations between coronal mass ejections and solar energetic proton events, *J. Geophys. Res.,* 1984, vol. 89, no. A11, pp. 9683–9694. https://doi.org/10.1029/JA089iA11p09683
7. Kahler, S.W., Injection profiles of solar energetic particles as functions of coronal mass ejection heights, *Astrophys. J.,* 1994, vol. 428, pp. 837–842.
8. Cliver, E., Kahler, S., and Vestrand, W., On the origin of gamma-ray emission from the behind limb flare on 29 September 1989, *23rd Int. Cosmic Ray Conf.,* 1993, vol. 3, pp. 91–94.
9. Bazilevskaya, G.A., Effects of coronal propagation of solar protons with energies above 100 *MeV, Izv. Akad. Nauk SSSR. Ser. Fiz.,* 1984, vol. 48, no. 11, pp. 2171–2173.
10. Klein, K.-L., Chupp, E.L., Trottet, G., et al., Flare-associated energetic particles in the corona and at 1 AU, *Astron. Astrophys.,* 1999, vol. 348, pp. 271–285.
11. Ackermann, M., Ajello, M., Albert, A., et al., High-energy gamma-ray emission from solar flares: Summary of *Fermi* large area telescope detections and analysis of two M-class flares, *Astrophys. J.,* 2014, vol. 787, no. 1. https://doi.org/10.1088/0004-637X/787/1/15
12. Ajello, M., Albert, A., Allafort, A., et al., Impulsive and long duration high-energy gamma-ray emission from the very bright 2012 March 7 solar flares, *Astrophys. J.,* 2014, vol. 789, no. 1, p. 20. https://doi.org/10.1088/0004-637x/789/1/20
13. Ajello, M., Baldini, L., Bastieri, R., et al., First Fermi-LAT solar flare catalog, *Astrophys. J. Suppl.,* 2021, vol. 252, p. 13. https://doi.org/10.3847/1538-4365/abd32e
14. Ackermann, M., Allafort, A., Baldini, L., et al., Fermi-LAT observations of high-energy behind-the-limb solar flares, *Astrophys. J.,* 2017, vol. 835, p. 219. https://doi.org/10.3847/1538-4357/835/2/219
15. Cliver, E.W., Flare versus shock acceleration of high-energy protons in solar energetic particle events, *Astrophys. J.,* 2016, vol. 832, p. 128. https://doi.org/10.3847/0004-637X/832/2/128
16. Gopalswamy, N., Yashiro, S., Makela, P., et al., The common origin of high-energy protons in solar energetic particle events and sustained gamma-ray emission from the Sun, *Astrophys. J.,* 2021, vol. 915, p. 82. https://doi.org/10.3847/1538-4357/ac004f
17. Struminskii, A.B., Grigor'eva I.Yu., Logachev, Yu.I., et al., Solar electrons and protons in the events of September 4–10, 2017 and related phenomena, *Plasma Phys. Rep.,* 2020, vol. 46, no. 2, pp. 174–188. https://doi.org/10.1134/S1063780X20020130
18. Struminsky, A.B., Grigor'eva, I.Yu., Logachev, Yu.I., et al., Two phases of solar flares and a stochastic mechanism for acceleration of electrons and protons, *Astrophysics,* 2020, vol. 63, no. 3, pp. 388–398.
19. Miller, J.A., Cargill, P.J., Emslie, A.G., et al., Critical issues for understanding particle acceleration in impulsive solar flares, *J. Geophys. Res.,* 1997, vol. 102, no. A7, pp. 14631–14660. https://doi.org/10.1029/97JA00976
20. Grigorieva, I.Yu. and Struminsky, A.B., Formation of sources for solar cosmic rays in eruptive flares X6.9 and M5.1 observed August 9, 2011, and May 17, 2012, *Astron. Rep.,* 2022, vol. 99, no. 6, pp. 481–489. https://doi.org/10.1134/S106377292206004X
21. Struminsky, A.B., Grigor'eva, I.Yu., Logachev, Yu.I., and Sadovski, A.M., Relationship between duration and rate of the CME acceleration, *Geomagn. Aeron. (Engl. Transl.),* 2021, vol. 61, no. 6, pp. 781–791. https://doi.org/10.1134/S0016793221050133
22. Struminsky, A.B., Grigorieva I.Yu., Logachev, Yu.I., and Sadovskii, A.M., Solar electrons and protons in flares with a pronounced impulsive phase, *Bull. Russ.*

Acad. Sci.: Phys., 2021, vol. 85, no. 8, pp. 907–910. https://doi.org/10.3103/S1062873821080281

23. Lysenko, A.L., Frederiks, D.D., Fleishman, G.D., et al., X-ray and gamma-ray emission from solar flares, *Phys.-Usp.,* 2020, vol. 63, no. 8, p. 818. https://doi.org/10.3367/UFNe.2019.06.038757
24. Gopalswamy, N. and Makela, P., Latitudinal connectivity of ground level enhancement events, *ASP Conf. Ser.,* 2013.
25. Cliver, E.W., Mekhaldi, F., and Muscheler, R., Solar longitude distribution of high-energy proton flares: Fluences and spectra, *Astrophys. J. Lett.,* 2020, vol. 900, p. L11. https://doi.org/10.3847/2041-8213/abad44
26. Winter, L.M., Bernstein, V., Omodei, N., et al., A statistical study to determine the origin of long-duration gamma-ray flares, *Astrophys. J.,* 2018, vol. 864, p. 39. https://doi.org/10.3847/1538-4357/aad3c0
27. Share, G.H., Murphy, R.J., White, S.M., et al., Characteristics of late-phase >100 MeV gamma-ray emission in solar eruptive events, *Astrophys. J.,* 2018, vol. 869, p. 182. https://doi.org/10.3847/1538-4357/aaebf7
28. de Nolfo, G.A., Bruno, A., Ryan, J.M., et al., Comparing long-duration gamma-ray flares and high-energy solar energetic particles, *Astrophys. J.,* 2019, vol. 879, p. 90. https://doi.org/10.3847/1538-4357/ab258f
29. Struminsky, A.B. and Zimovets, I.V., Time of arrival of the first relativistic solar protons to the Earth, *Bull. Russ. Acad. Sci.: Phys.,* 2009, vol. 73, no. 3, pp. 315–318.
30. Grechnev, V.V., Kiselev, V.I., Uralov, A.M., et al., An updated view of solar eruptive flares and the development of shocks and CMEs: History of the 2006 December 13 GLE-productive extreme event, *Publ. Astron. Soc. Jpn.,* 2013, vol. 65, p. S9. https://doi.org/10.1099/pasj/65.sp1.S9
31. Papaioannou, A., Kouloumvakos, A., Mishev, A., et al., The first ground-level enhancement of solar cycle 25 on 28 October 2021, *Astron. Astrophys.,* 2022, vol. 660, p. L5. https://doi.org/10.1051/0004-6361/202142855
32. Mishev, A.L., Kocharov, L.G., Koldobskiy, S.A., et al., High resolution spectral and anisotropy characteristics of solar protons during the GLE №73 on 28 October 2021 derived with neutron monitor analyses, *Sol. Phys.,* 2022, vol. 298, no. 7, p. 88. https://doi.org/10.1007/s11207-022-02026-0
33. Gopalswamy, N., Xie, H., Akiyama, S., et al., The first ground level enhancement event of solar cycle 24: Direct observation of shock formation and particle release heights, *Astrophys. J.,* 2013, vol. 765, p. L30. https://doi.org/10.1088/2041-8205/765/2/L30
34. Gopalswamy, N., Yashiro, S., Thakur, N., et al., The 2012 July 23 backside eruption: An extreme energetic particle event?, *Astrophys. J.,* 2016, vol. 833, no. 2, p. 216. https://doi.org/10.3847/1538-4357/833/2/216
35. Gopalswamy, N., Yashiro, S., Makela, P., et al., Extreme kinematics of the 2017 September 10 solar eruption and the spectral characteristics of the associated energetic particles, *Astrophys. J.,* 2018, vol. 863, no. 2, p. L39. https://doi.org/10.3847/2041-8213/aad86c
36. Omodei, N., Pesce-Rollins, M., Longo, F., et al., Fermi-LAT observations of the 2017 September 10 solar flare, *Astrophys. J.,* 2018, vol. 865, p. L7. https://doi.org/10.3847/2041-8213/aae077
37. Thakur, N., Gopalswamy, N., Xie, H., et al., Ground level enhancement in the 2014 January 6 solar energetic particle event, *Astrophys. J.,* 2014, vol. 790, p. L13. https://doi.org/10.1088/2041-8205/790/1/L13
38. Gopalswamy, N., Mäkelä, P., and Yashiro, S., Particle acceleration and transport at the sun inferred from Fermi/LAT observations of >100 MeV gamma-rays, *Proc. AOGS 2021 (18th Annual Meeting of the Asia Oceania Geosciences Society),* 2021, ArXiv:2108.11286.
39. Kocharov, L., Omodei, N., Mishev, A., et al., Multiple sources of solar high-energy protons, *Astrophys. J.,* 2021, vol. 915, no. 1, p. 12. https://doi.org/10.3847/1538-4357/abff57
40. Pesce-Rollins, M., Omodei, N., Krucker, S., et al., The coupling of an EUV coronal wave and ion acceleration in a Fermi-LAT behind-the-limb solar flare, *Astrophys. J.,* 2022, vol. 929, p. 172. https://doi.org/10.3847/1538-4357/ac5f0c
41. Bieber, J.W., Clem, J., Evenson, P., et al., A maverick GLE: The relativistic solar particle event of December 13, 2006, *Proc. 30th Int. Cosmic Ray Conf.,* 2008, vol. 1, pp. 229–232.
42. Klein, K.-L., Musset, S., Vilmer, N., et al., The relativistic solar particle event on 28 October 2021: Evidence of particle acceleration within and escape from the solar corona, *Astron. Astrophys.,* 2022, vol. 663, p. A173. https://doi.org/10.1051/0004-6361/202243903
43. Chertok, I.M., On some features of the solar proton event on 2021 October 28—GLE73, *Mon. Not. R. Astron. Soc.,* 2022, vol. 517, no. 2, pp. 2709–2713. https://doi.org/10.1093/mnras/stac2843
44. Li, X., Wang, Y., Guo, J., et al., Solar energetic particles produced during two fast coronal mass ejections, *Astrophys. J. Lett.,* 2022, vol. 928, p. L6. https://doi.org/10.3847/2041-8213/ac5b72
45. Struminsky, A.B., Multiple acceleration of protons on the Sun and their free propagation to the Earth on January 20, 2005, *Astron. Lett.,* 2006, vol. 32, no. 10, pp. 688–697.
46. Reames, D.V., Solar release times of energetic particles in ground-level events, *Astrophys. J.,* 2009, vol. 693, pp. 812–821. https://doi.org/10.1088/0004-637X/693/1/812
47. Reames, D.V., Solar energetic-particle release times in historic ground-level events, *Astrophys. J.,* 2009, vol. 706, pp. 844–850. https://doi.org/10.1088/0004-637X/706/1/844

Translated by M. Chubarova